



Orientation influence on grain size effects in ultrafine-grained magnesium

Haidong Fan,^{a,b,*} Sylvie Aubry,^c A. Arsenlis^c and Jaafar A. El-Awady^a

^aDepartment of Mechanical Engineering, Johns Hopkins University, Baltimore, MD 21218, USA

^bDepartment of Mechanics, Sichuan University, Chengdu, Sichuan 610065, People's Republic of China

^cCondensed Matter and Materials Division, Lawrence Livermore National Laboratory, Livermore, CA 94551-0808, USA

Received 4 September 2014; revised 21 October 2014; accepted 28 October 2014

The mechanical behavior of ultrafine-grained magnesium was studied by discrete dislocation dynamics (DDD) simulations. Our results show basal slip yields a strong size effect, while prismatic and pyramidal slips produce a weak one. We developed a new size–strength model that considers dislocation transmission across grain boundaries. Good agreement between this model, current DDD simulations and previous experiments was observed. These results reveal that the grain size effect depends on three factors: Peierls stress, dislocation source strength and grain boundary strength.

© 2014 Acta Materialia Inc. Published by Elsevier Ltd. All rights reserved.

Keywords: Discrete dislocation dynamics; Grain size effects; Ultrafine-grained magnesium; Orientation

As the lightest structural metal, magnesium and its alloys are utilized in many applications in automotive, aerospace and other industries. Due to the low symmetry of hexagonal close-packed (hcp) crystals, Mg and its alloys display a strong anisotropic behavior [1], especially in Mg polycrystals having a strong texture. Size-strengthening in polycrystalline Mg can be characterized into three groups according to the texture [2]: (i) weak grain size effects for basal textured polycrystals tested in tension with the *c*-axis under contraction, resulting in deformation by compression twinning, pyramidal and prismatic slips [2,3]; (ii) intermediate size effects during the deformation of weak/random textured polycrystals, deforming through basal slip and tension twinning [3–5]; and (iii) strong size effects in basal texture tested in compression with the *c*-axis under tension, which leads to predominant tension twinning deformation [6–8]. The different intensities of the orientation dependent size effects are similar to face-centered cubic (fcc; strong effect) and body-centered cubic (bcc; weak effect) materials [9], and were attributed to the variations in the Peierls stress [10]. However, this conflicts with the Hall–Petch relationship, which assumes a constant power law exponent of -0.5 that is independent of the Peierls stress. That is to say, the Hall–Petch relationship does not address the effect of orientation or texture directly.

Here we conduct a parametric study on the influence of orientation on the grain size effects of ultrafine-grained Mg

using three-dimensional discrete dislocation dynamics (3D-DDD) simulator, ParaDiS [11,12]. Figure 1(a) shows the representative cubical simulation cell, having edge length *d*, with periodic boundary conditions (PBCs) along three directions. All six surfaces of the simulation cell are considered as grain boundaries (GBs). The cell size is varied between 800 nm and 1.5 μm . The basic Mg properties chosen for the simulations are: shear modulus, $G = 17$ GPa; Poisson ratio, $\nu = 0.29$; magnitude of the $\langle a \rangle$ dislocation Burgers vector, $b = 0.325$ nm; axial ratio, $c/a = 1.6236$; and mass density, $\rho = 1738$ kg m $^{-3}$.

Twinning has always been observed in polycrystalline Mg, but is strongly dependent on grain size. In AZ31, Barnett et al. [13] showed that the stress–strain response changes from a concave shape to a convex one when the grain size is ~ 4 μm , indicating the absence of twinning deformation for such small grain sizes. Lapovok et al. [14] pointed out that the transition grain size below which twinning is absent is 3–4 μm for ZK60. More recently, Li et al. [8] revealed that the transition grain size in pure magnesium polycrystals is about 2.7 μm , below which dislocation slip dominates. Many studies show that twinning exhibits a stronger grain size effect than dislocation slip in fcc, bcc and hcp materials [15]. That is to say, the critical stress to activate twinning increases faster with decreasing grain size. As a result, there exists a transition grain size below which dislocation slip dominates. Based on the aforementioned experimental observations, the transition grain size is ~ 3 μm , which is consistent with the grain size studied here. Accordingly, twinning can be safely ignored in the current polycrystalline DDD simulations.

* Corresponding author at: Department of Mechanical Engineering, Johns Hopkins University, Baltimore, MD 21218, USA; e-mail addresses: haidongfan8@foxmail.com; jelawady@jhu.edu

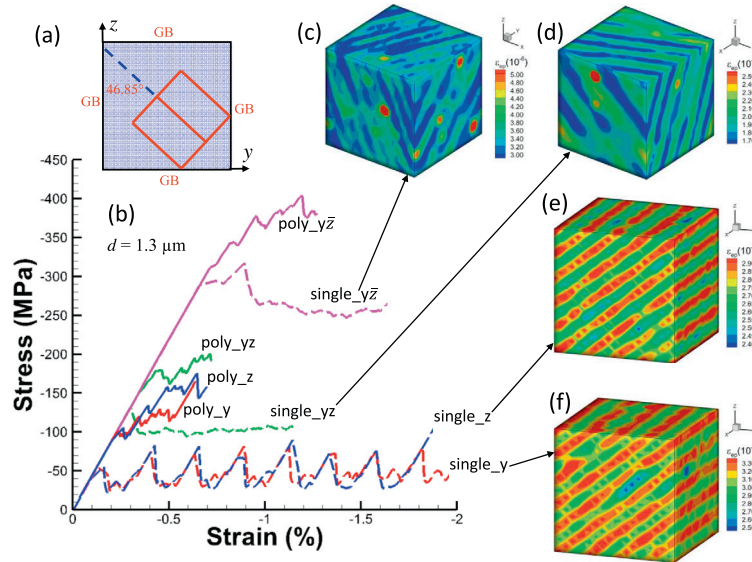


Figure 1. (a) 2D schematic of the simulation cell on the yz plane. (b) Stress–strain responses from single crystalline and polycrystalline simulations under different loading orientations. The insets (c)–(f) are contours of effective plastic strain showing active slip traces in the single crystal simulations.

The grain orientation was chosen such that the c -axis makes a 46.85° angle with respect to the z -axis of the simulation cell (see Fig. 1(a)). Using this representative grain model, the orientations of all the grains in the bulk materials are identical, corresponding to the strong basal texture in polycrystalline Mg. However, the misorientation between the a -axes in neighboring grains is not accounted for here. Nevertheless, the GB is introduced as a nominal interface/barrier to dislocation motion. Dislocations trapped at the GB can be transmitted into neighboring grains if the shear stress on the dislocation exceeds the GB strength, as adopted by previous DDD simulations of polycrystalline fcc materials [16]. The GB transmission strength is largely governed by the misorientation angle, i.e. $\tau_{GB} = 2G\sin^2(0.5\theta_{mis})$ [17–19]. The experimental characteristics of as-received pure Mg show that the majority of GBs are low-angle GB, while for equal-channel angular pressed Mg samples the fraction of high-angle GBs exceeds that of low-angle GBs after the eighth pass [20]. Thus, we chose an intermediate case with a nominal misorientation angle, $\theta_{mis} = 15^\circ$, and nominal GB transmission strength, $\tau_{GB} = 580$ MPa.

Initially, Frank–Read (FR) dislocation sources of length $l_{src} = 800b$ were randomly distributed within the simulation cell, with an initial dislocation density of $\rho_{src} = 5 \times 10^{12} \text{ m}^{-2}$. The slip system of each FR source was chosen randomly to have either an $\langle a \rangle$ Burgers vector on the basal, prismatic or pyramidal I planes or a $\langle c + a \rangle$ Burgers vector on pyramidal II planes. These slip systems typically produce most of the dislocation-mediated plasticity in Mg [21,22], and have been commonly chosen in previous crystal plasticity and DDD simulations [12,23]. To account for possible statistics of dislocation distributions, each grain size was simulated using at least three different initial dislocation distributions. The experimentally measured Peierls stresses for dislocations on the basal (0.52 MPa), prismatic (39.2 MPa) and pyramidal (105 MPa) planes have been prescribed in previous simulations [24]. Finally, since the c -axis resides in the yz plane, deformation under four representative loading orientations was investigated: (i) along the (010) direction, or y

loading; (ii) along (001), or z loading; (iii) along (011), or yz loading; and (iv) along (01 $\bar{1}$), or $y\bar{z}$ loading. The strain rate imposed in all simulations was $\dot{\epsilon} = -5000 \text{ s}^{-1}$.

The compressive stress–strain responses of the $d = 1.3 \mu\text{m}$ grain loaded in the four loadings are shown in Figure 1(b). The responses of single crystal simulations are also shown for comparison. In Figure 1(c)–(f), the effective plastic strain contours show the active slip traces from single crystal simulations. While twinning was reported in single crystals [25,26], it is not considered here due to the difficulties in incorporating twinning plasticity in current DDD simulations. Nevertheless, single crystal simulations are beneficial to revealing the deformation modes under different loading directions. Besides, comparison with the polycrystalline simulations qualitatively addresses the effect of GBs on dislocation-mediated plasticity.

The single crystal responses under y and z loadings are effectively similar, since these directions make angles of 46.85° and 43.15° with respect to the basal plane. Thus, plasticity is mostly facilitated by basal slip, as evidenced in Figure 1(e–f). Furthermore, these responses are distinct, with multiple stress drops followed by elastic loading intervals, which could be linked to source nucleation [19], since basal dislocations have low Peierls stress and high mobility. On the other hand, under yz and $y\bar{z}$ loadings, the Mg single crystal exhibits higher yield and flow stresses. The yz loading axis is nearly perpendicular to the c -axis, and plasticity is predominantly accommodated by prismatic slip, as shown in Figure 1(d). The $y\bar{z}$ loading axis nearly coincides with the c -axis and pyramidal II slip dominates. Recent hcp 2D-DDD simulations are qualitatively consistent with the current single crystal simulations [27]. For polycrystals, similar increases in the strength as a function of loading orientation are also observed. Finally, while all the single crystal simulations show no hardening, a strong hardening is observed from all the polycrystal simulations, as a direct consequence of GB strengthening.

Figure 2 shows the yield stress vs. grain size for different loading orientations. In order to investigate the orientation dependence of the size effect intensity, a power law $\sigma_y \propto d^{-n}$

is used to fit the results. The prismatic and pyramidal slip-dominated orientations exhibit a weak grain size effect, with an exponent $n \approx 0.2$, which agrees well with experimental results [2]. On the other hand, the basal slip orientation demonstrates a much stronger size effect, with an exponent $n = 1.16$. Experimental studies suggested that the orientation influence is mainly driven by anisotropy in the Peierls stresses [2]. To investigate this, the Peierls stress contribution $\sigma_0 = \tau_0/P$ (τ_0 is the Peierls stress, P is the Schmid factor) was subtracted from the yield stress to formulate a “Hall–Petch” power law relationship in the form $(\sigma - \sigma_0) \propto d^{-n}$, as shown in Figure 2(b). The exponent for pyramidal slip changes from 0.2 to 0.52, and for prismatic slip from 0.22 to 0.42. These exponents are still considerably lower than that for basal slip, conveying that anisotropy in the Peierls stress alone cannot explain the orientation dependence, and that other factors influencing grain size effects must be accounted for.

Many GB modeling studies have shown that dislocation transmission across GBs plays an important role in the overall mechanical behavior [17–19,28], which has also often been observed experimentally [29,30]. Therefore, the polycrystal yielding can be characterized by two conditions: (i) activation of pre-existing dislocation sources (grain yielding); and (ii) dislocation transmission across a GB due to dislocation pileups (GB yielding). The latter can be expressed mathematically as:

$$k\tau_y = \tau_{GB} \quad (1)$$

where τ_y is yield shear stress or critical resolved shear stress (CRSS) and k is the number of dislocations in the pileup. Furthermore, a dislocation source at the grain center will experience a back stress τ_b from dislocation pileups at the

GB. Thus, the shear stress required to activate a source can be expressed as

$$\tau_{src} = \tau_y - \tau_b \quad (2)$$

where τ_{src} is the dislocation source activation strength. In the following, we assume that the length of the dislocation pileups is considerably smaller than the grain size, so that the distance between the dislocation source and any pileup dislocation is approximately $d/2$. Thus, the back stress from the pileups is

$$\tau_b = 4kD/d \quad (3)$$

where $D = Gb/2\pi(1 - \nu)$. Solving Eqs. (1)–(3), the yield strength can be expressed as:

$$\tau_y = \frac{1}{2}(\tau_{src} + \sqrt{\tau_{src}^2 + 16D\tau_{GB}/d}) \quad (4)$$

Eq. (4) is a dislocation pileup and transmission model that accounts for the strength of pre-existing sources as well as the GB strength. When τ_{src} is low (large grains) or τ_{GB} is high (high-angle GBs),

$$\tau_y \approx \tau_{src} + 2\sqrt{D\tau_{GB}}d^{-0.5} \quad (5)$$

which is equivalent to the traditional Hall–Petch relationship. On the other hand, if $\tau_{GB} = 0$, then the yield strength is governed only by the strength of pre-existing dislocation sources, $\tau_y = \tau_{src}$, which is the case of single crystals. In general, both τ_{src} and τ_{GB} should be accounted for adequately. The dislocation source strength can be expressed by [31,32]

$$\tau_{src} = \tau_0 + \beta Gb\sqrt{\rho_{dis}} + \alpha Gb/\bar{\lambda}_{max} \quad (6)$$

where $\bar{\lambda}_{max}$ is the statistical maximum dislocation source length, which is also a function of grain size [16]. Thus, the grain size effect depends on three factors: Peierls stress, dislocation source activation stress and GB strength. $\bar{\lambda}_{max}$ and its standard deviation for polycrystalline materials were given in Ref. [16] by:

$$\bar{\lambda}_{max} = \int_0^d P(\lambda_{max})\lambda_{max}d\lambda_{max} \quad (7)$$

$$\sigma_{\lambda_{max}} = \left(\int_0^d P(\lambda_{max})\lambda_{max}^2d\lambda_{max} - \bar{\lambda}_{max}^2 \right)^{1/2} \quad (8)$$

here, $P(\lambda_{max}) = n \frac{4(d-2\lambda_{max})}{d^2} \left(1 - \frac{(d-2\lambda_{max})^2}{d^2} \right)^{n-1}$, the number of dislocation pinning points $n = 2 \text{ integer}[r_{mob}\rho_{src}V/l_{src}]$, and r_{mob} is the percentage of mobile dislocations. A similar model was also used for single crystalline magnesium [33].

The proposed model is plotted in Figure 3 vs. the current DDD simulations and some published experimental results. In the model, the following parameters were used [34]: $\beta = 0.35$; $\alpha = 0.6$; and $r_{mob} = 1/12$, $1/6$ and $1/4$ for basal, prismatic and pyramidal slips, respectively. It is clear from Figure 3(a) that the proposed dislocation pileup and transmission model agrees well with the current DDD simulations. Both DDD and the model show a stronger size effect for basal slip. In Figure 3(a), the single-arm source model for polycrystalline materials (only Eqs. (6)–(8) without consideration of dislocation transmission across GBs) [16] is also shown. It is clear that this model on its own fails to capture the grain size effects, indicating that dislocation transmission across GBs plays an important role in the response of ultrafine-grained Mg and cannot be ignored.

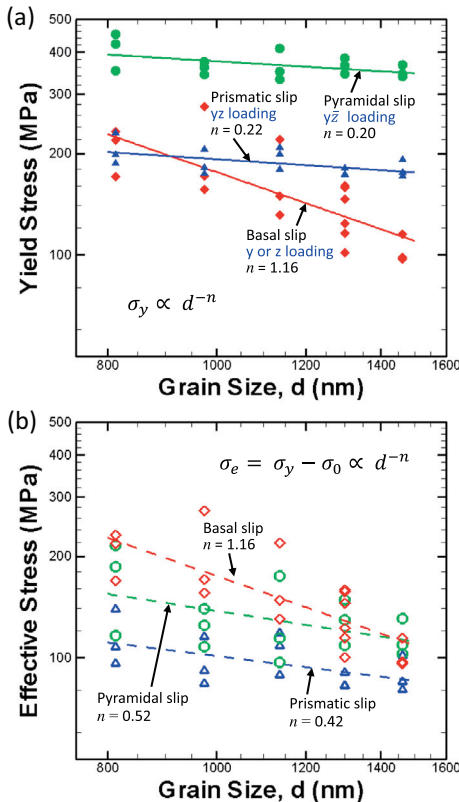


Figure 2. (a) Yield stress σ_y and (b) effective stress $\sigma_e = \sigma_y - \sigma_0$ as a function of grain size, d , under different loading directions.

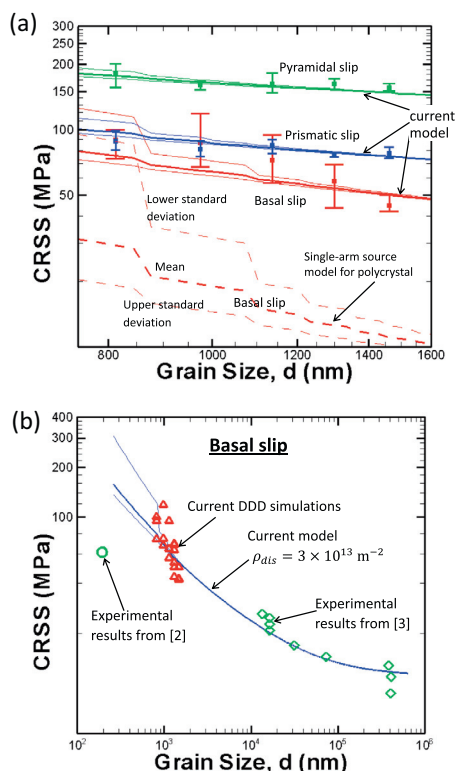


Figure 3. Grain size effects on CRSS as predicted from: (a) DDD simulations, current model and single-arm source model; and (b) DDD simulations, current model and experiments for basal slip.

Figure 3(b) shows that the current model and DDD simulations agree well with experimental predictions, with the exception of a single experimental point for grain size below 200 nm. This could be due to the deformation mechanisms other than dislocation pileup and transmission in such a size regime, like GB sliding [6] and stress-driven grain growth [35].

In summary, discrete dislocation dynamics simulations were employed to investigate the orientation and grain size effects in ultrafine-grained Mg. A strong size effect was observed for basal slip, while weak ones were found for prismatic and pyramidal slips. A new dislocation pileup and transmission model was also developed, which shows that the grain size effect is a function of three factors: Peierls stress, dislocation source strength and grain boundary strength. Finally, good agreement between this model, DDD simulations and published experimental results was observed.

This research was sponsored by the Army Research Laboratory (#W911NF-12-2-0022). The views and conclusions contained in this document are those of the authors and should not be interpreted as representing the official policies, either expressed or implied, of ARL or the US government. The US government is authorized to reproduce and distribute reprints for governmental purposes notwithstanding any copyright notation herein. H.F. also gratefully acknowledges the financial support of Natural Science Foundation of China (11302140).

- [1] E.W. Kelley, W.F. Hosford, The plastic deformation of magnesium : technical report, (1967).
- [2] J.A. Sharon, Y. Zhang, F. Momprou, M. Legros, K.J. Hemker, *Scr. Mater.* 75 (2014) 10–13.
- [3] D.V. Wilson, J.A. Chapman, *Philos. Mag.* 8 (1963) 1543–1551.
- [4] G.S. Rao, Y.V.R.K. Prasad, *Metall. Mater. Trans. A* 13 (1982) 2219–2226.
- [5] N. Ono, R. Nowak, S. Miura, *Mater. Lett.* 58 (2004) 39–43.
- [6] H.J. Choi, Y. Kim, J.H. Shin, D.H. Bae, *Mater. Sci. Eng., A* 527 (2010) 1565–1570.
- [7] Z. Trojanová, Z. Szárász, A. Mielczarek, P. Lukáč, W. Riehemann, *Mater. Sci. Eng., A* 483–484 (2008) 477–480.
- [8] J. Li, W. Xu, X. Wu, H. Ding, K. Xia, *Mater. Sci. Eng., A* 528 (2011) 5993–5998.
- [9] J.R. Greer, J.T.M. De Hosson, *Prog. Mater. Sci.* 56 (2011) 654–724.
- [10] A.S. Schneider, C.P. Frick, B.G. Clark, P.A. Gruber, E. Arzt, *Mater. Sci. Eng., A* 528 (2011) 1540–1547.
- [11] A. Arsenlis, W. Cai, M. Tang, M. Rhee, T. Oppelstrup, G. Hommes, T.G. Pierce, V.V. Bulatov, *Model. Simul. Mater. Sci. Eng.* 15 (2007) 553–595.
- [12] C.C. Wu, P.W. Chung, S. Aubry, L.B. Munday, A. Arsenlis, *Acta Mater.* 61 (2013) 3422–3431.
- [13] M.R. Barnett, Z. Keshavarz, A.G. Beer, D. Atwell, *Acta Mater.* 52 (2004) 5093–5103.
- [14] R. Lapovok, P.F. Thomson, R. Cottam, Y. Estrin, *J. Mater. Sci.* 40 (2005) 1699–1708.
- [15] M.A. Meyers, O. Vöhringer, V.A. Lubarda, *Acta Mater.* 49 (2001) 4025–4039.
- [16] C. Zhou, R. LeSar, *Int. J. Plast.* 30–31 (2011) 185–201.
- [17] H. Fan, Z. Li, M. Huang, X. Zhang, *Int. J. Solids Struct.* 48 (2011) 1754–1766.
- [18] Z. Li, C. Hou, M. Huang, C. Ouyang, *Comput. Mater. Sci.* 46 (2009) 1124–1134.
- [19] H. Fan, Z. Li, M. Huang, *Scr. Mater.* 66 (2012) 813–816.
- [20] S. Biswas, S. Singh, S. Suwas, *Acta Mater.* 58 (2010) 3247–3261.
- [21] Y. Tang, J.A. El-Awady, *Acta Mater.* 71 (2014) 319–332.
- [22] S.R. Agnew, Ö. Duygulu, *Int. J. Plast.* 21 (2005) 1161–1193.
- [23] J. Zhang, S.P. Joshi, *J. Mech. Phys. Solids* 60 (2012) 945–972.
- [24] S. Groh, E.B. Marin, M.F. Horstemeyer, D.J. Bammann, *Model. Simul. Mater. Sci. Eng.* 17 (2009) 075009.
- [25] K.E. Prasad, K. Rajesh, U. Ramamurty, *Acta Mater.* 65 (2014) 316–325.
- [26] Q. Yu, L. Qi, K. Chen, R.K. Mishra, J. Li, A.M. Minor, *Nano Lett.* 12 (2012) 887–892.
- [27] S. Olarnrithinun, S.S. Chakravarthy, W.A. Curtin, *J. Mech. Phys. Solids* 61 (2013) 1391–1406.
- [28] B. Liu, D. Raabe, P. Eisenlohr, F. Roters, A. Arsenlis, G. Hommes, *Acta Mater.* 59 (2011) 7125–7134.
- [29] Z. Shen, R.H. Wagoner, W.A.T. Clark, *Acta Metall.* 36 (1988) 3231–3242.
- [30] T.C. Lee, I.M. Robertson, H.K. Birnbaum, *Philos. Mag. A* 62 (1990) 131–153.
- [31] T.A. Parthasarathy, S.I. Rao, D.M. Dimiduk, M.D. Uchic, D.R. Trinkle, *Scr. Mater.* 56 (2007) 313–316.
- [32] H. Fan, Z. Li, M. Huang, *Scr. Mater.* 67 (2012) 225–228.
- [33] J. Zhang, K.T. Ramesh, S.P. Joshi, *Model. Simul. Mater. Sci. Eng.* 22 (2014) 075003.
- [34] S.I. Rao, D.M. Dimiduk, M. Tang, T.A. Parthasarathy, M.D. Uchic, C. Woodward, *Philos. Mag.* 87 (2007) 4777–4794.
- [35] Y. Zhang, J.A. Sharon, G.L. Hu, K.T. Ramesh, K.J. Hemker, *Scr. Mater.* 68 (2013) 424–427.